Lifescience Global

Journal of Coating Science and Technology
http://www.lifesciencesglobal.com/journals/journal-of-coating-science-and-technology

Reactively Magnetron Sputter-Deposited Ti (C,N) Nanocomposite Thin Films: Composition and Thermal Stability

Osama A. Fouad[1,*], Hong-Ying Lin[2] and S. Ismat Shah[3]

[1]*Central Metallurgical Research and Development Institute, CMRDI. P.O. Box: 87 Helwan 11421, Cairo, Egypt*

[2]*Department of Civil and Environmental Engineering, University of Delaware, Newark DE, 19716, USA*

[3]*Department of Physics and Astronomy and Material Science and Engineering, University of Delaware, Newark DE, 19716, USA*

Abstract: Titanium carbonitride thin films were grown by reactive magnetron sputtering deposition of titanium carbide target in Ar/N_2 gas mixture on p-type silicon (100) substrates. With the increase of sputtering power up to 125W, the deposition rate and films thickness reached a maximum of 14nm/min and 430nm, respectively. A thick film of about 2200nm could be deposited for 120 min at the optimum deposition pressure of 20mTorr. Cathode current decreased from about 290mA to reach a value of about 235mA as the N_2 flow percentage increased from 0 to 100%. X-ray diffraction analyses of the deposited films confirmed the formation of titanium carbide and carbonitride layers as the nitrogen gas concentrations in the process gas were increased. SEM image of the deposited titanium carbonitride thin film for 5 min deposition time showed that the film started to grow as tiny particles of size as low as about 140nm, which in later stage coalesced together to form bigger grains and finally a continuous film. The deposited film shows good thermal stability upon annealing in air and in vacuum at 700°C for 2 hours.

Received on 01-09-2018
Accepted on 26-10-2018
Published on 12-11-2018

Keywords: Titanium carbonitride, Nanocomposite thin films, Reactive magnetron sputtering, Thermal stability.

DOI: https://doi.org/10.6000/2369-3355.2018.05.02.2

1. INTRODUCTION

Fabrication of multicomponent nanocomposite films by reactive sputtering technique has been studied by several research groups. The periodic arrangement of such materials in a multilayer structure in a nanoscale can result in the growth of a well compositionally modified structure for vital applications. Reactive sputtering is a commonly used technique for film growth of metal oxides, nitrides, and carbides, etc., [1-4]. Usually, in this process, a metal target is sputtered in a mixture of argon and one or more reactive gases such as oxygen, nitrogen, methane, etc. [5-7]. However, despite its great advantages over sputtering compound targets, reactive sputter deposition from metallic targets often exhibit several obstacles in controlling the stoichiometry of the films. This is due to instabilities in the reactive gas pressure near the metal-to-compound transition region and differential poisoning of magnetron sputtering cathode target as a result of the formation of an electrically less conductive layer on its surface. Indeed, it requires a critical control of the process parameters such as gas flow rate and pressure to produce films with reproducible composition [6,8]. To overcome these obstacles, additional costs represented by increasing pumping speed, larger vacuum chamber to increase the target-to-substrate distance and continuous monitoring must be taken into consideration to optimize the process. On the other hand, it is hard to sputter a compound target and the sputtering yield and consequently the deposition rate is usually quite low.

Titanium carbonitride (TiCN) thin films as a single phase are a promising material combining several important properties such as high hardness and high thermal stability. This stability came from the fact that all transition-metal carbides including titanium carbide (TiC) have a very large stability range and a significant amount of carbon vacancies. They are characterized by low thermal conductivity, high melting point, high hardness, and pronounced nonstoichiometry which gives the ability to tune the physical properties of the films without structural transitions [4,7]. On the other hand, titanium nitride thin films are widely used for a variety of structural as well as functional applications such as wear resistant, decorative and microelectronics applications due to its hardness, lustrous golden yellow color, and good electrical conductivity, and good diffusion barrier characteristics.

*Central Metallurgical Research and Development Institute, CMRDI. P.O. Box: 87 Helwan 11421, Cairo, Egypt; Tel: (202)- 2714-2454; Fax: (202)- 2714-2451; E-mail: oafouad@yahoo.com

E-ISSN: 2369-3355/18

Combining these advantages in one compound might lead to a unique property functional material [9].

Several works have been done for the deposition of TiC films including reactive sputtering [10] activated reactive evaporation [11], ion beam implantation [12], vacuum arc deposition [13] and magnetron sputtering of Ti followed by plasma nitriding of carburized steel [14]. On the other hand, the most commonly used technique for the deposition of TiN thin films is reactive sputtering from an elemental Ti target using a sputtering gas mixture consisting of Ar and N_2 [9]. Here in we report on reactive magnetron sputtering deposition of Ti (C,N) thin films using titanium carbide target in Ar/N_2 gas mixture. The parameters affecting the process such as sputtering power, deposition pressure and time, and N_2/Ar flow rate ratio have been investigated. The deposited films have been characterized for their crystal structure and chemical composition and the results obtained are explored.

2. EXPERIMENTAL

2.1. Materials

P-type B-doped Si (100) 1 × 1cm dimensions pieces have been used as substrates. Ar and N_2 research purity gases (99.99%) have been used as process and reactive gas respectively. Titanium carbide compound 5.08 cm disk was used as a sputtering target.

2.2. System Set-Up and Procedure

The films were deposited on silicon substrates by reactive magnetron sputtering in a turbo pumped stainless steel chamber. Details on the sputtering system have been published previously [15]. Prior to each experiment, the target was sputtered in presence of pure Ar gas for 30 min to recover its surface conditions. After the cleaning process, substrate shutter was opened and the N_2 gas was introduced into the deposition chamber and its flow rate was gradually increased. Then the cathode current was allowed to stabilize before recording its value. The parameters affecting the sputtering process have been studied such as power (50-200W), deposition time (5-125min), deposition pressure (15-30mTorr) and N_2/Ar flow rate ratio. The drop in cathode current due to introducing N_2 gas to the process gas was also monitored and recorded. Films deposition was also carried out at each gas flow point and the produced films were characterized physicochemically.

2.3. Process Diagnosis and Films Characterization

Process diagnosis was performed through follow up of changing in target electrical characteristics such as current and voltage. Deposition rates and films thickness were calculated using a Sloan Dektak IIA profilometer. The crystal structure of the deposited films and phase identification were investigated by XRD using a Rigaku D-Max B diffractometer equipped with a graphite crystal monochromator. XRD θ-2θ scans were performed using Cu-K_α (λ= 1.5405Å) radiation in the 2θ range from 30° to 80° at room temperature. Surface morphology of the as-deposited films was investigated by SEM using scanning electron microscopy JEOL-JSM-7400F operating at an accelerating voltage of 100V to 30kV with a resolution of 1.5nm at 1kV. The chemical composition of the as-deposited and thermally annealed deposited films were determined using XPS survey scans which performed on an SSI 310 X-probe spectrometer using Al K_α radiation at 1486.6eV. The sample surfaces were lightly etched, prior to the XPS analyses, using 100eV Ar^+ ion for 5 min to remove any surface contaminations.

3. RESULTS AND DISCUSSION

When TiC target is sputtered in presence of N_2 reactive gas in presence of Ar process gas grey-black color thin films are deposited on Si substrates and the target itself. Films' color and consequently composition were mainly affected by the gas type, flow rates, pressure, and sputtering power.

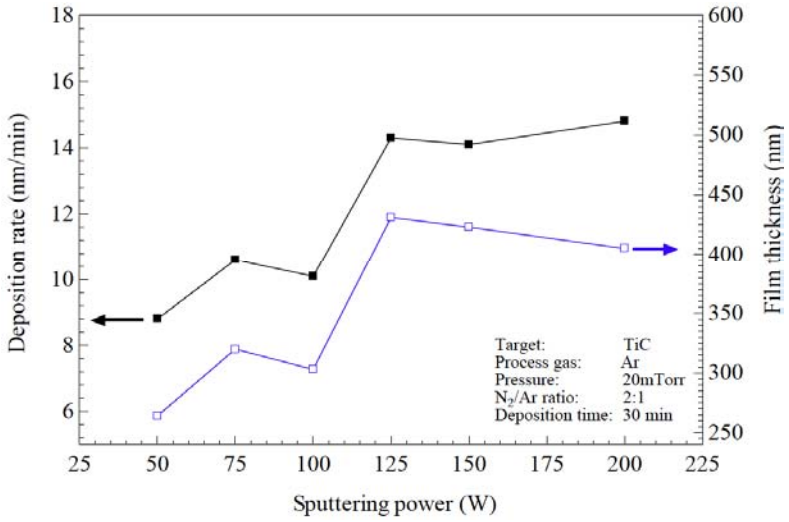

Figure 1: Deposition rate and film thickness as a function of sputtering power.

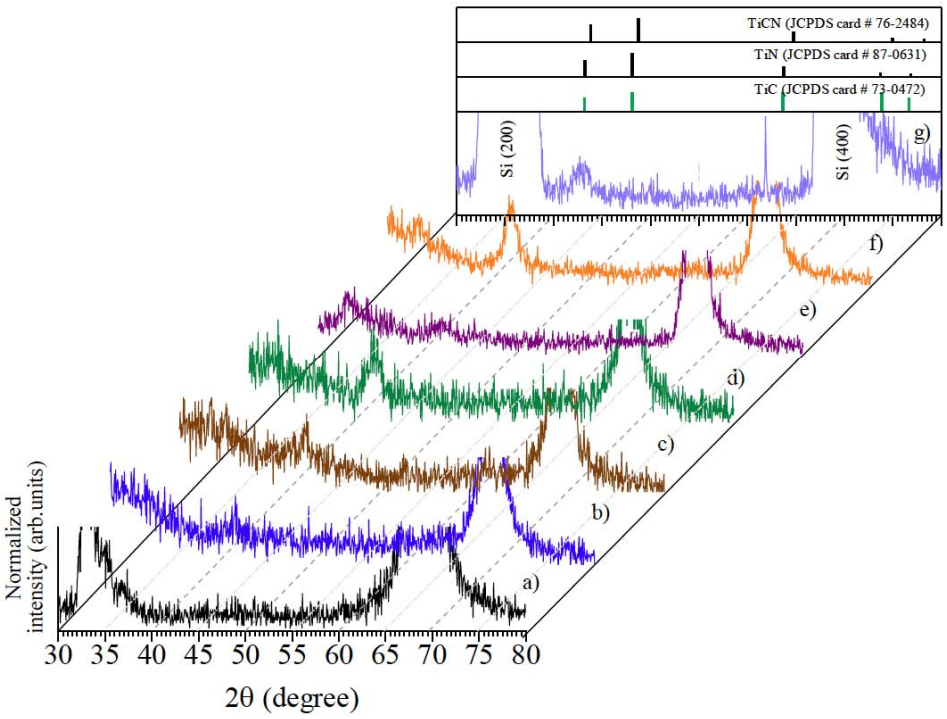

Figure 2: XRD patterns of the as-deposited Ti (C,N) films at various sputtering power (**a**) Si substrate, (**b**) 50 W, (**c**) 75 W, (**d**) 100 W, (**e**) 125 W, (**f**) 150 W and (**g**) 200 W.

3.1. Sputtering of TiC Compound Target

3.1.1. Effect of Sputtering Power

Figure **1** shows the variation of deposition rate together with the variation in film thickness as a function of sputtering power. It is clear that as the sputtering power increased from 50 up to 125W, whereas the deposition rate increased from about 9nm/min to reach a value of about 14nm/min. Further increase in sputtering power up to 200 W did not significantly change the deposition rate. These results are comparable with the film thickness increment to about 430nm upon increasing of sputtering power up to 125W. As the sputtering power increased above 125W and up to 200W, the film thickness decreased to about 400nm. The slight decrease in film thickness might be due to the etching of the produced film by the generated plasma at such higher sputtering power.

Figure **2** shows the XRD patterns with normalized intensities of the deposited films at various sputtering power at the deposition time of 30min. The XRD patterns of pure silicon substrate (Figure **2a**) and the stick XRD patterns of the corresponding phases are also shown for comparison. It is obvious that the diffraction peaks corresponding to Si (200) and Si (400) planes are detected for the pure silicon substrate. Figures **2b**, **c**, **d**, **e**, **f**, and g are the XRD patterns of the deposited films at 50, 75, 100, 125, 150 and 200W, respectively. The films are deposited in presence of nitrogen and argon gases at a flow rate ratio of 2:1, respectively. The diffraction peaks characteristic to TiC (JCPDS card # 73-0472) and TiN phases (JCPDS card # 87-0631) appeared at 2θ of 41.67 and 60.51°, respectively. These peaks detected in all patterns with a little shift toward higher 2θ values upon increasing the sputtering power up to 150W. At sputtering power of 200 W a sharp shift in the peak positions to 42.58 and 61.98°, respectively is observed implying the formation of TiCN phase (JCPDS card # 76-2434).

3.1.2. Effect of Sputtering Time

The effect of sputtering (deposition) time was studied at 125 W sputtering time, N_2:Ar flow at the ratio of 2:1 (66 % N_2 flow rate concentration) at a total pressure of 20mTorr. Figure **3** shows the variation in deposition rates and films thickness as a function of the deposition time intervals. It is obvious that as the deposition time increased from 5 to 30 min, the deposition rate decreased from about 38 to 14nm/min, respectively. Further increase in deposition time up to 120min did not affect the deposition rate significantly. The decrease of the deposition rate with time might be due to target poisoning as a result of the formation of titanium carbonitride layer at target surface which lowers the sputtering rate. The thick film can be obtained up to 2200nm thick as the deposition time increased to 120min.

Normalized XRD patterns of the as-deposited films at different deposition time intervals are represented in Figure **4**. XRD pattern of Si substrate is also shown there for comparison, Figure **4a**. The XRD patterns of the as-deposited films at, 5, 15, 30, 60, 75, 90, and 120 min are represented in Figures **4b**, **c**, **d**, **e**, **f**, **g**, and **h**, respectively. The characteristic diffraction peak of TiC phase at 2θ of 41.78° can be easily seen in all patterns. However the one at 2θ of 61.19° that characteristic of the TiCN phase is observed for

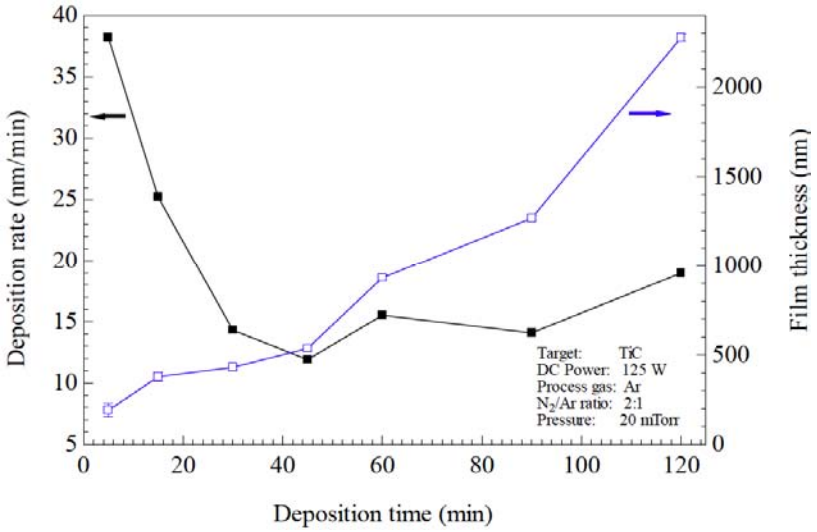

Figure 3: Deposition rate and film thickness as a function of deposition time.

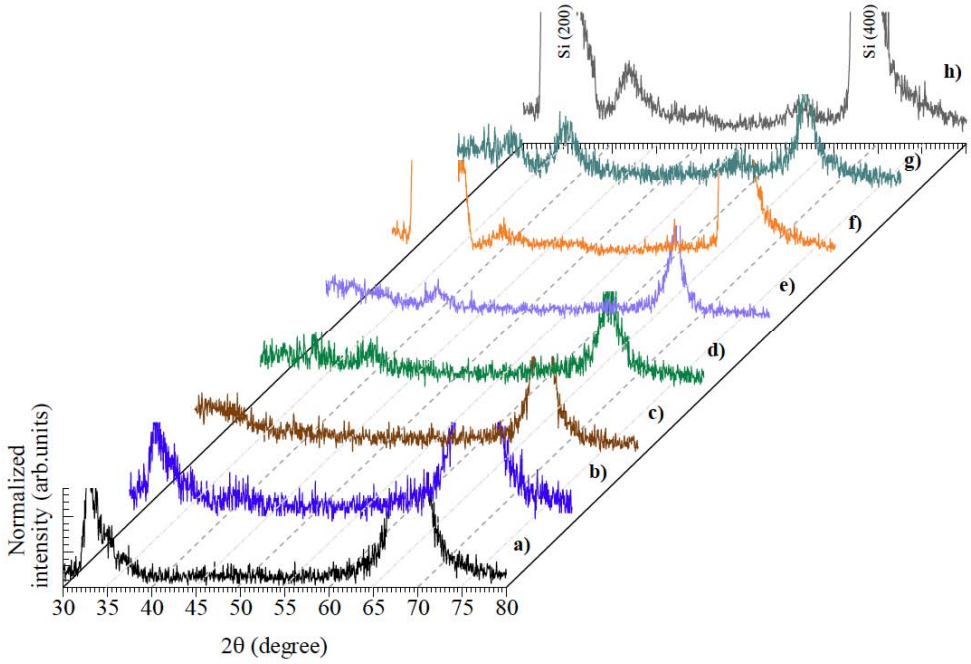

Figure 4: XRD patterns of the as-deposited Ti (C,N) films at various deposition time (**a**) Si substrate, (**b**) 5 min, (**c**) 15 min, (**d**) 30 min, (**e**) 60 min, (**f**) 75 min, (**g**) 90 min and (**h**) 120 min.

the films deposited at longer deposition time. This might be due to the amorphous nature of the deposited films which can be overcome by the deposition of thick films.

3.1.3. Effect of Deposition Pressure

Figure **5** shows the variation of deposition rate and film thickness as a function of deposition total pressure. It is clear that as the deposition pressure increased from 15 to 20mTorr, the deposition rate increased from 30 nm/min to about 40 nm/min, respectively. As the deposition pressure increased to 25mTorr, the deposition rate slightly decreased to about 35nm/min. Further increase in deposition pressure to 30mTorr led to a sharp decrease in the deposition rate to reach a value of about 15nm/min. On the other hand, film thickness reached a maximum of 220nm as the deposition pressure increased from 15 to 25mTorr. A dramatic decrease in film thickness to a value of about 95nm is observed as the deposition pressure increased to 30mTorr. The sharp decrease in both deposition rate and film thickness upon increasing the deposition pressure might be due to the formation of titanium carbon nitride layer which is hard to sputter than the carbide layer itself The XRD patterns of the film deposited at various deposition pressures are in agreement with these results, Figure **6**. The diffraction peak assigned for TiCN phase at 2θ of 61.69^{o} is detected for the film deposited at 25mTorr, Figure **6c**. The target poisoning by

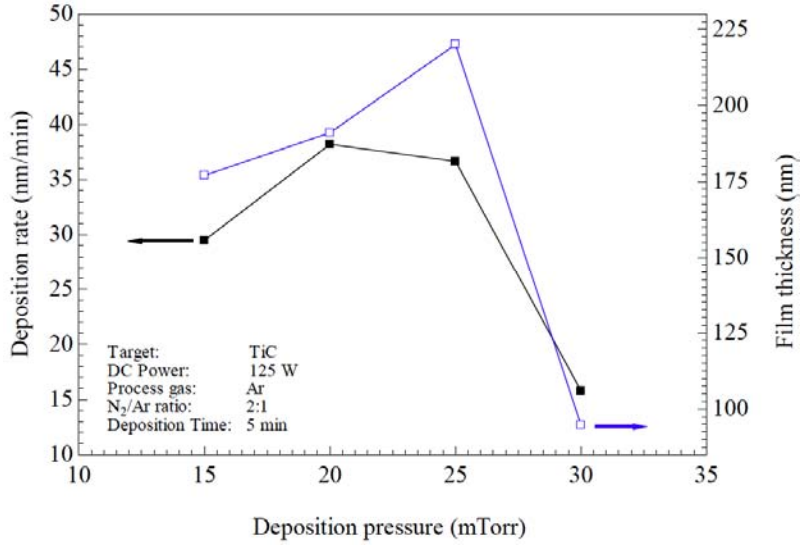

Figure 5: Deposition rate and film thickness as a function of deposition pressure.

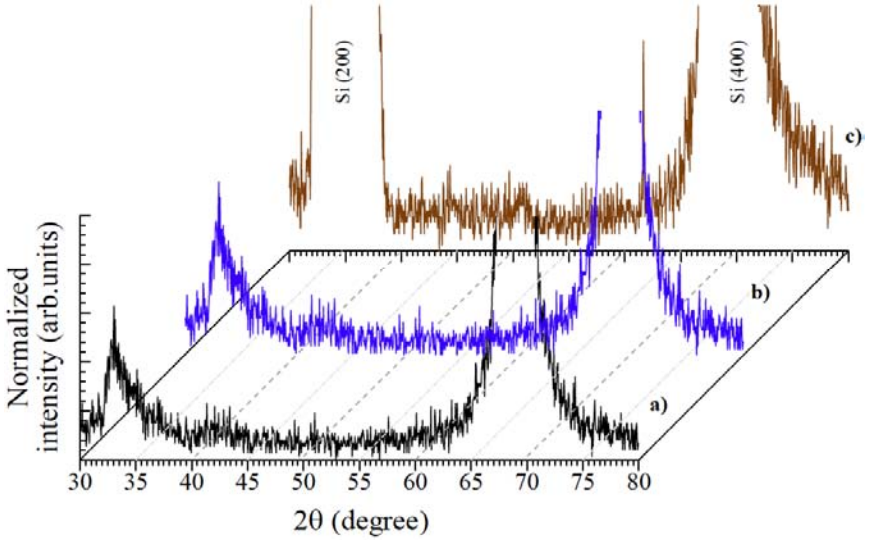

Figure 6: XRD patterns of the as-deposited Ti (C,N) films at various deposition pressure (**a**) 15 mTorr, (**b**) 20 mTorr, (**c**) and 25 mTorr.

the deposition of the TiCN layer might be the reason of lower deposition rate and/or film thickness at higher deposition pressure (> 25mTorr).

3.1.4. Effect of N_2/Ar Flow Rate Ratio

Figure **7** represents the variation in cathode current upon increasing the N_2 gas flow rate ratio. It is clear that as the N_2 flow rate percentage increased from 0 to 100 %, the cathode current decreased from about 345 to reach a value of about 235 mA, respectively. These results are comparable with that obtained from the XRD patterns of the deposited films, Figure **8**. As can be clearly seen the characteristic peak at 2θ of 61.76^{o} corresponding to TiCN phase increased as the N_2 flow rate percentage increased up to 85 %. However, its intensity is diminished or reduced as the N_2 flow rate parentage increased to 100 % where the sputtering of fully poisoned target became hard. This might be due to the fact that the difference between the electronegativities of Ti (1.54) and N (3.04) compared to Ti and C (2.55) leads to the formation of strongly bonded titanium carbonitride films at higher N_2 flow rate concentration percentage. The binding energy between Ti, C, and N is the result of lower sputtering yield and a sharp drop in cathode current. It has been concluded by another research group that the type and ratio of the reactive gas led to a preferred orientation in reactively sputter deposited nanocrystalline TiN thin films [9]. However, the diminish of the peak intensity at high N_2 flow rate concentration confirmed its relation with the status of the target surface and does not affect the structure ad orientation considerably under our experimental conditions.

Figure **9** shows the SEM image of the deposited TiCN film at early stages after 5 min deposition time at 15 mTorr deposition pressure, 125 W power and 1:1 of N_2:Ar flow rate ratio (50 % N_2 flow rate concentration) using titanium carbide

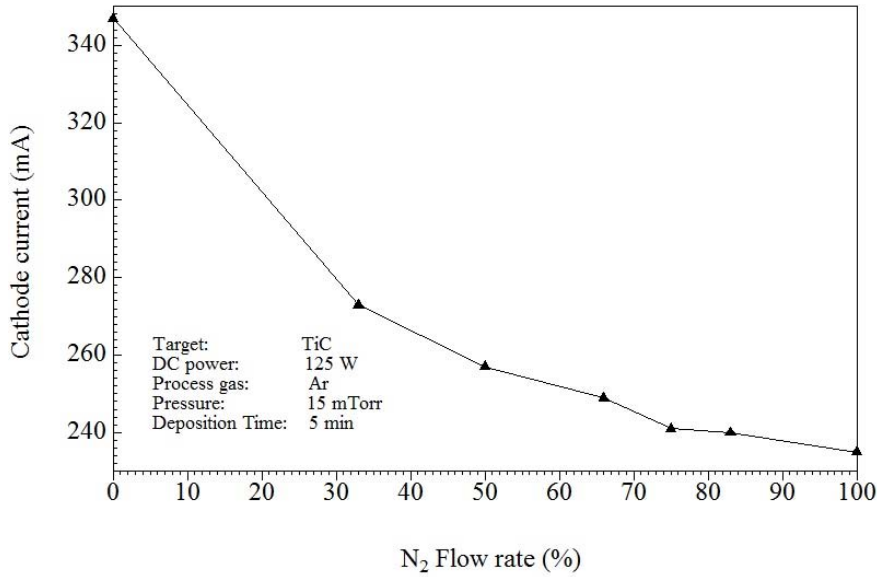

Figure 7: Target (cathode) current variation versus nitrogen flow rate concentration.

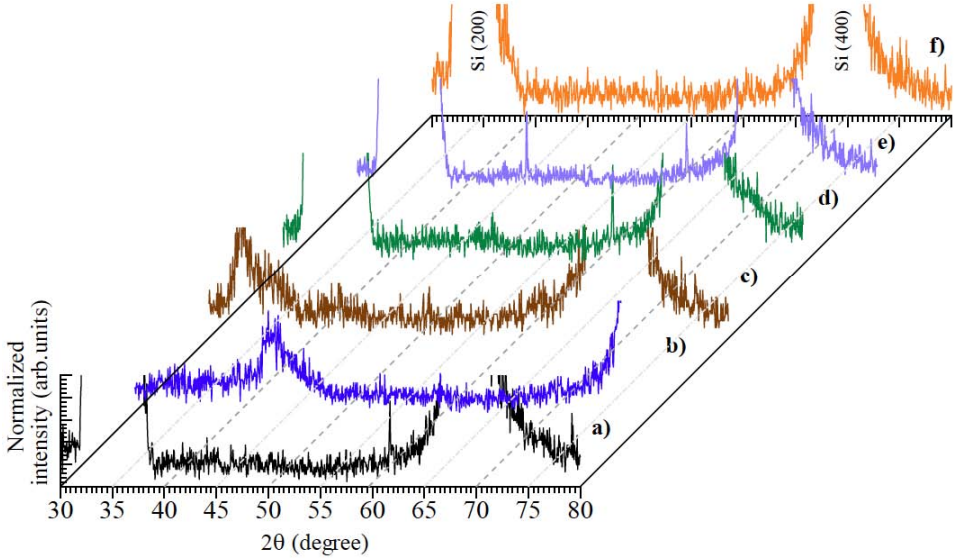

Figure 8: XRD patterns of the as-deposited Ti (C,N) films at various N_2 flow rate concentrations (**a**) 33 %, (b) 50 %, (**c**) 66 %, (**d**) 75 %, (**e**) 83 % and (**f**) 100 %.

target. It is clear that the films firstly deposited in the form of nanocrystalline droplets or tiny particles of size as low as 140 nm (dashed circle) at the initial nucleation stage. Later on, these nanocrystals are propagated (oval circle) and coalesced to form elongated microcrystalline crystals (solid-line rectangular). Then at the final deposition stage, the microcrystals form a continuous microcrystalline film. The upper right inset shows the early growth stages. The surface morphology investigation indicates that the continuous film grows by a lateral growth mechanism at the later deposition stage [16].

3.1.5. Effect of Vacuum and Air Annealing

Figure **10** shows the XRD patterns of the as-deposited film at 125W, 20mTorr, 2:1 N_2/Ar flow ratio for 30min and the annealed films in a vacuum (6.84 x 10^{-5} Torr) and in the air at 700°C for 2hrs. No observable change in the XRD patterns can be detected. To confirm the stability of the films, XPS survey and high resolution scan in the range of Ti_{2P}, C_{1S} and N_{1S} peaks are investigated for the as-deposited film and that annealed in vacuum, Figure **11**. The presented XPS peaks are of normalized intensity. Ti_{2P}, C_{1S} and N_{1S} peaks detected at 460.23, 287.07 and 397.42eV, respectively [17]. The remarkable shift in binding energy for Ti, C, and N is indicating that they are in a compound form rather than elemental form. Oxygen contamination is confirmed by the presence of an O_{1S} peak at 532.23eV. This oxygen is believed to be on the film surface and did not affect the bulk composition of the film. This result is in agreement with that obtained from XRD where no titanium oxide phase can be

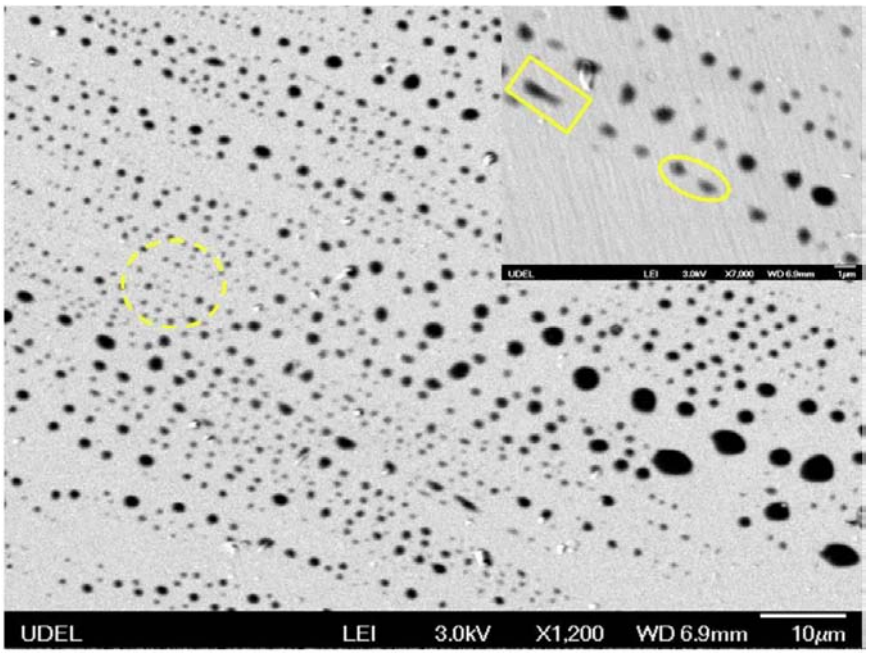

Figure 9: SEM image of the as-deposited Ti (C,N) at the early deposition stage at 15 mTorr deposition pressure, N_2/Ar flow ratio of 1:1, 15 W sputtering power for 5 min deposition time.

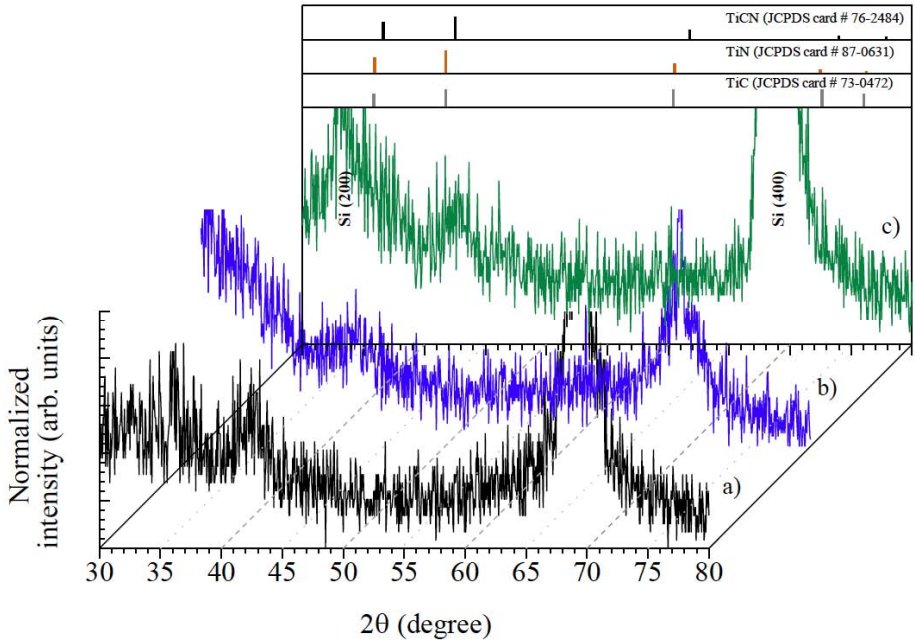

Figure 10: XRD patterns of the deposited Ti (C,N) films (**a**) as-deposited at 125 W, 20 mTorr, 2:1 N_2/Ar flow ratio for 30 min (**b**) sample (**a**) annealed in vacuum (6.84×10^{-5} Torr) at 700 °C for 2 hrs and (**c**) annealed in air at 700 °C for 2 hrs.

detected. Detailed investigation of Ti, C, and N peaks confirmed that Ti peaks are splatted into two peaks. The peak at 459.08eV is ascribed to $Ti_{2P3/2}$ state whereas that at 464.82eV is attributed to $Ti_{2P1/2}$ state. No observable chemical shifts are detected in the peaks position in the two samples except that a small shift to a higher state is observed for the Ti_{2P} peak in the annealed sample. This might be due to the formation of a more dense film upon heating whereas the number of vacancies is decreased.

4. CONCLUSIONS

Reactive magnetron sputtering of titanium carbide target in Ar as a process gas at various additions of reactive nitrogen gas has been investigated. The sputtering process was diagnosed by monitoring the cathode current which shows an observable decrease from 345mA to 235mA as the reactive gas flow rate concentrations increased from 0 to 100%., respectively. The XRD analyses confirmed the formation of

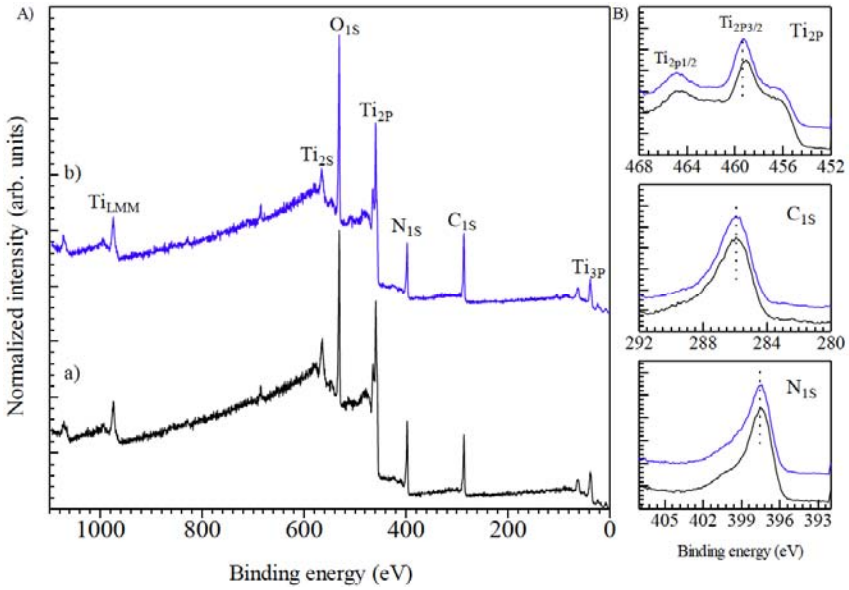

Figure 11: XPS (**A**) survey and (**B**) high resolution scans of the deposited Ti (C,N) films mentioned in Figure **10** (**a**) as-deposited film (**b**) annealed at 700 ^{o}C for 2hrs.

titanium carbide (TiC) phase and titanium carbonitride phase at higher sputtering power > 75W, 20mTorr and lower N_2 flow rate concentration < 100%. While sputtering power increased from 50 to 125W increased the deposition rate from about 8.5 to 14nm/min, the increase in deposition time from 5 to 30min decreased the deposition rate from about 38 to 14nm/min. Optimum deposition pressure was found to be 20mTorr for titanium carbide (TiC) target sputtering. SEM image of the deposited film from sputtering TiC target at N_2/Ar flow rate ratio of 1:1 for 5min showed that the film is mainly composed of tiny particles of size as low as 140nm.

ACKNOWLEDGEMENT

This work was supported by the Junior Scientist Development Visit Grants Program, U.S.-Egypt Joint Board on Scientific and Technological Cooperation, Ministry of Scientific Research, Egypt.

REFERENCES

[1] Safi I. Recent aspects concerning DC reactive magnetron sputtering of thin films: a review. Surf Coat Technol 2000; 127: 203-218. https://doi.org/10.1016/S0257-8972(00)00566-1

[2] Kelly PJ, Arnell RD. Magnetron sputtering: a review of recent developments and applications. Vacuum 2000; 56: 159-172. https://doi.org/10.1016/S0042-207X(99)00189-X

[3] Stueber M, Holleck H, Leiste H, Seemann K, Ulrich S, Ziebert C. Concepts for the design of advanced nanoscale PVD multilayer protective thin films. J Alloys Compd 2009; 483: 321-333. https://doi.org/10.1016/j.jallcom.2008.08.133

[4] Pierson HO. Handbook of refractory carbides and nitrides. Noyes Publications 1996.

[5] Fouad OA, Ali B, Shah SI. Hysteresis, structural and composition characteristics of deposited thin films by reactively sputtered titanium target in Ar/CH_4/N_2 gas mixture. Mater Sci Technol 2013; 29: 985-989. https://doi.org/10.1179/1743284713Y.0000000240

[6] Sproul WD, Chritie DJ, Carter DC. Control of reactive sputtering processes. Thin Solid Films 2005; 491: 1-17. https://doi.org/10.1016/j.tsf.2005.05.022

[7] Eklund P, Ph.D. Thesis, Linköping University, Linköping, Sweden, 2007.

[8] Waite MM, Shah SI. Reactive sputtering of silicon with oxygen and nitrogen. Mater Sci Eng B 2007; 140: 64-68. https://doi.org/10.1016/j.mseb.2007.04.001

[9] Banerjee R, Chandra R, Ayyub P. Influence of the sputtering gas on the preferred orientation of nanocrystalline titanium nitride thin films. Thin Solid Films 2002; 405: 64-72. https://doi.org/10.1016/S0040-6090(01)01705-9

[10] Senna LF, Achete CA, Hirsch T, Freire FL Jr. Structural, chemical, mechanical and corrosion resistance characterization of TiCN coatings prepared by magnetron sputtering. Surf Coat Technol 1997; 94-95; 390-397. https://doi.org/10.1016/S0257-8972(97)00447-7

[11] Chen JY, Yu GP, Huang JH. Corrosion behavior and adhesion of ion-plated TiN films on AISI 304 steel. Mater Chem Phys 2000; 65: 310-315. https://doi.org/10.1016/S0254-0584(00)00255-8

[12] Kim SK, Kim TH, Whole J, Rie K-T. TiCN Coatings on aluminum alloy formed by MO-PACVD. Surf Coat Technol 2000; 131: 121-126. https://doi.org/10.1016/S0257-8972(00)00831-8

[13] Ren CS, Mu ZX, Wang YN, Yu H. Surf Coat Technol 2004; 185: 210. https://doi.org/10.1016/j.surfcoat.2003.12.030

[14] Yang Y, Guo JH, Yan MF, Zhu YD, Zhang YX, Wang YX. Improvement of wear resistance for carburised steel by Ti depositing and plasma nitriding. J Surf Eng 2018; 34: 132-138. https://doi.org/10.1080/02670844.2016.1231863

[15] Fouad OA, Abdul Rumaiz K, Ismat Shah S. Reactive sputtering of titanium in Ar/CH_4 gas mixture: Target poisoning and film characteristics. Thin Solid Films 2009; 517: 5689-5694. https://doi.org/10.1016/j.tsf.2009.02.119

[16] Li TQ, Noda S, Tsuji Y, Ohsawa T, Komiyama H. Initial growth and texture formation during reactive magnetron sputtering of TiN on Si.(111). J Vac Sci Technol A 2002; 20: 583-588. https://doi.org/10.1116/1.1458944

[17] Fouad OA, Yamazato M, Ichinose H, Nagano M. Titanium disilicide formation by rf plasma enhanced chemical vapor deposition and film properties. Appl Surf Sci 2003; 206: 159-166. https://doi.org/10.1016/S0169-4332(02)01210-2